Nanotechnology **19** (2008) 295704 (5pp) doi:10.1088/0957-4484/19/29/295704

Time-resolved photoluminescence of type-II Ga(As)Sb/GaAs quantum dots embedded in an InGaAs quantum well

J Tatebayashi[1], B L Liang[1], R B Laghumavarapu[2], D A Bussian[3], H Htoon[3], V Klimov[3], G Balakrishnan[1], L R Dawson[2] and D L Huffaker[1,2]

[1] Electrical Engineering and California NanoSystems Institute, University of California, Los Angeles, 420 Westwood Plaza, Los Angeles, CA 90095, USA
[2] Center for High Technology Materials, University of New Mexico, 1313 Goddard SE, Albuquerque, NM 87106, USA
[3] Los Alamos National Laboratory, C-PCS MS J567, Los Alamos, NM 87545, USA

E-mail: tatebaya@ee.ucla.edu and huffaker@ee.ucla.edu

Received 11 February 2008, in final form 15 May 2008
Published 10 June 2008
Online at stacks.iop.org/Nano/19/295704

Abstract
Optical properties and carrier dynamics in type-II Ga(As)Sb/GaAs quantum dots (QDs) embedded in an InGaAs quantum well (QW) are reported. A large blueshift of the photoluminescence (PL) peak is observed with increased excitation densities. This blueshift is due to the Coulomb interaction between physically separated electrons and holes characteristic of the type-II band alignment, along with a band-filling effect of electrons in the QW. Low-temperature (4 K) time-resolved PL measurements show a decay time of $\simeq$40–70 ns from the transition between Ga(As)Sb QDs and InGaAs QW which is longer than that of the transition between Ga(As)Sb QDs and GaAs two-dimensional electron gas ($\simeq$30 ns).

1. Introduction

Ga(As)Sb/GaAs quantum dots (QDs) have recently attracted scientific interest because of their staggered (type-II) band alignment, wide band-gap range, and large valence band offset [1, 2], along with the zero-dimensional density of states (DOS) [3]. So far, several groups have reported the optical properties and carrier dynamics in type-II Ga(As)Sb QDs grown by molecular beam epitaxy (MBE) [4–13] or metalorganic chemical vapor deposition [14, 15]. Above all, incorporation of type-II QDs into a type-I quantum well (QW) offers intriguing optical properties due to their possible extended emission wavelength over 1.6 μm because of their large offsets of both conduction- and valence-bands. [13] Indeed, a combination of Ga(As)Sb/GaAs QDs and an InGaAs QW enables the wide range of emission wavelengths up to 1.7 μm according to 8-band $\mathbf{k}\cdot\mathbf{p}$ calculations [16]. This 'W'-like configuration allows a large flexibility to alter the wavefunction distribution of holes in the QW without significantly affecting the wavefunction of the holes inside the QD [17]. Type-II QDs could also be useful for single carrier, even unipolar storage devices including optical memory owing to their longer decay time caused by spatially separated electrons and holes. Several groups have reported the carrier dynamics of type-II Ga(As)Sb/GaAs QDs by means of time-resolved photoluminescence (TRPL), showing a decay time ($\simeq$10 ns) which is longer than that of type-I InAs/GaAs QDs ($<$1 ns) [6, 8]. This QD structure may have application in optoelectronic devices including lasers [13], detectors and solar cells [18] operating at the near-infrared or even mid-wavelength-infrared regimes. Our group has reported the lasing operation at room-temperature from 5-stacked Ga(As)Sb QDs in $In_{0.13}Ga_{0.87}As$ QWs at 1.026 μm [13]. However, there has been no report of the carrier dynamics of type-II QDs embedded in a type-I InGaAs QW. In this paper, we investigate the optical properties and carrier dynamics in type-II Ga(As)Sb/GaAs QDs embedded in an InGaAs QW by means of low-temperature photoluminescence (LTPL) and TRPL.

2. Experiments

All samples are grown by solid-source MBE on (100) semi-insulating GaAs substrates. After the growth of 100 nm

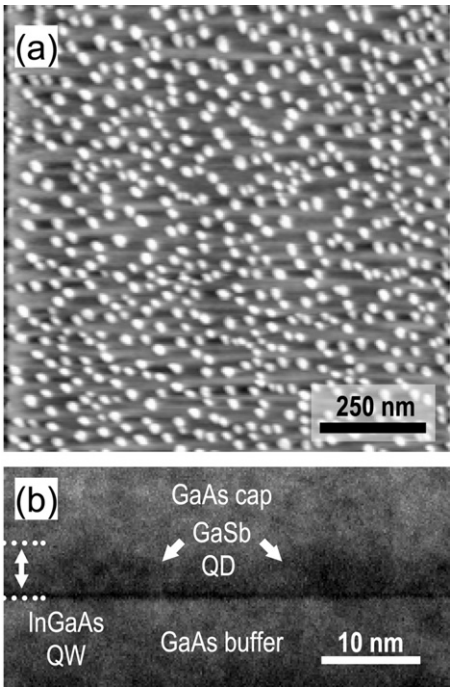

Figure 1. (a) AFM image of surface Ga(As)Sb QDs (dot density: 3.0×10^{10} cm^{-2}). (b) Cross-sectional TEM image of Ga(As)Sb QDs embedded in InGaAs QW.

GaAs buffer layer, two different types of single-stack Ga(As)Sb/GaAs QD structures are grown; the QDs capped with a 100 nm GaAs (structure (I)), and the QDs embedded in a 7 nm $In_{0.3}Ga_{0.7}As$ QW followed by a 100 nm GaAs cap (structure (II)). The growth rate, V/III ratio, and nominal thickness of QDs are 0.32 monolayers (MLs) s^{-1}, 1, and 4 ML, respectively. The QD density is determined to be 3.0×10^{10} cm^{-2} by atomic force microscope (AFM) as shown in figure 1(a). Figure 1(b) shows the cross-sectional transmission electron microscope (TEM) image indicating QDs embedded in the QW and sandwiched between GaAs buffer and cap. The width and height of QDs are estimated to be approximately 15 and 8 nm, respectively. From the structure (I), a transition pathway can be expected between a hole in Ga(As)Sb QDs and an electron confined in the two-dimensional electron gas (2DEG) at the GaAs/Ga(As)Sb interface (3De–0Dh) as shown in figure 2(a). On the other hand, from the structure (II), one additional transition pathway can be expected which includes more strongly confined electrons to a ring-like wavefunction in the QW surrounding QDs (2De–0Dh transition) as shown in figure 2(b) [13]. Such an identification of transition pathways can be also elucidated by the photoreflectance measurements along with eight-band $\mathbf{k} \cdot \mathbf{p}$ calculations [16]. LTPL and TRPL spectra for both of the structures (I) and (II) are collected using a conventional PL setup with an excitation by continuous-wave semiconductor lasers and Ti:sapphire lasers (repetition rate of 9 MHz) at pumping wavelengths (λ_{pump}) of 730 and 785 nm under measurement temperatures of 8 and 4 K, respectively.

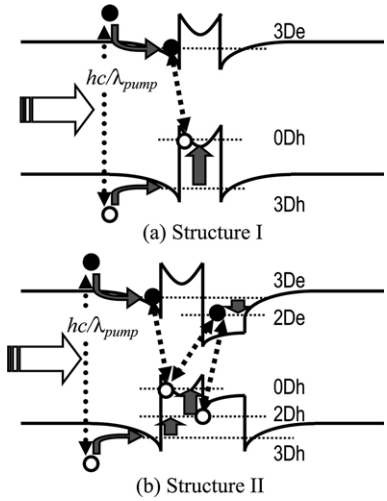

Figure 2. Schematic band diagram of type-II Ga(As)Sb/GaAs QDs (a) capped with GaAs (structure (I)) and (b) embedded in an InGaAs QW (structure (II)).

3. Results and discussions

Figure 3(a) shows the LTPL spectra of these two samples with different excitation densities ranging from 19 mW cm^{-2} to 24 W cm^{-2}. A single PL peak at 1.17 eV is observed from the structure (I) at very low excitation density, and likely originates from the 3De–0Dh transition. No PL from the excited states of QDs is observed because of the overlap of hole energy states caused by the small energy separation of each hole energy state in type-II Ga(As)Sb QDs and the large inhomogeneous broadening which results from the size distribution of SK QDs [16]. The PL spectrum of the structure (II) shows the existence of two peaks at 1.06 and 1.19 eV corresponding to the 2De–0Dh and 3De–0Dh transitions, respectively. On the other hand, no PL from the InGaAs QW (2De–2Dh transition) is observed even at a higher excitation density indicating that the probability of the 2De–2Dh transition is extremely small because of hole relaxation from QW to QDs. It is noted that the observed PL peak energy is much larger than expected from the theoretical values because of intermixing of Arsenic adatoms into QDs (25–50%) due to the interdiffusion of adatoms while growing cap layers at comparatively high-temperature (510 °C) [16]. Figure 3(b) plots the peak energy of each PL peak (3De–0Dh transition of the structure (I), 3De–0Dh and 2De–0Dh transition of the structure (II)) with different excitation densities. The observed blueshift is due to the band bending or distortion caused by the Coulomb interaction between physically separated excitons which is characteristic of the type-II band alignment [4, 6–11]. The band-filling of holes in the QD-DOS leads to an additional shift of the PL maximum energy to higher energies. On the other hand, a larger blueshift ($\simeq$76 meV) of the PL peak from the 2De–0Dh transition compared with that from the 3De–0Dh transition is observed under the same excitation density. Such a larger blueshift can be caused by a subsequent band-filling effect of electrons confined in the QW at higher excitation density, along with the band bending by Coulomb interaction of excitons.

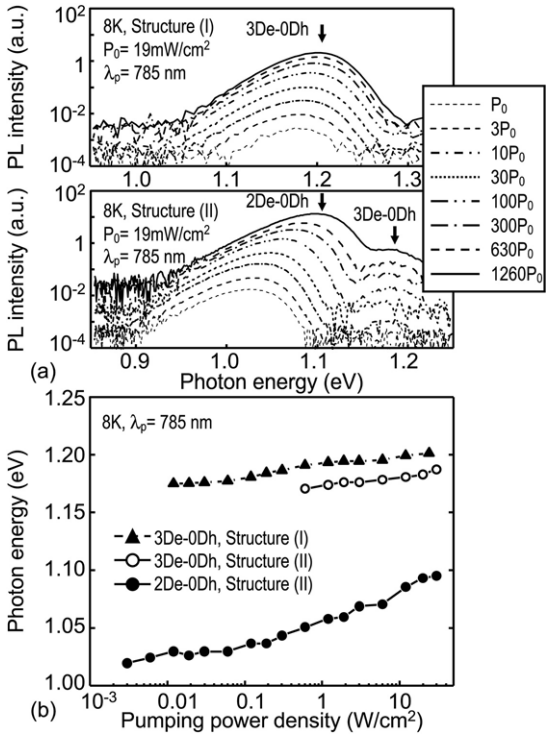

Figure 3. (a) LTPL spectra of the structure (I) and (II) at different excitation densities ranging from 19 mW cm^{-2} to 24 W cm^{-2}. (b) Photon energy of each peak of Ga(As)Sb QDs capped with GaAs or $In_{0.3}Ga_{0.7}As$ QW versus excitation densities.

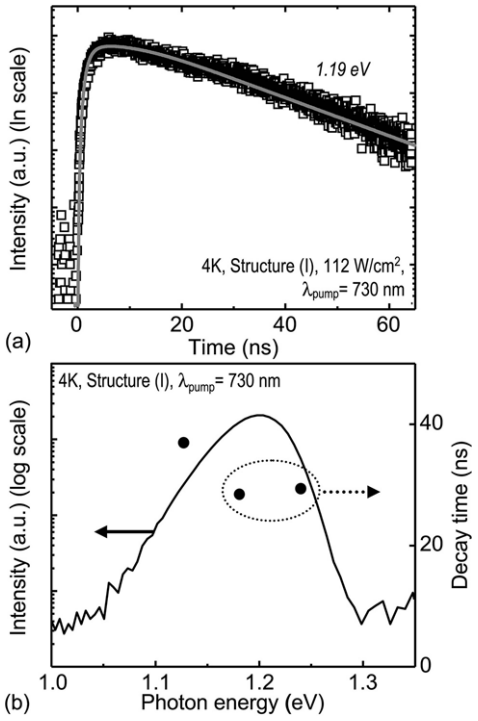

Figure 4. (a) Decay curves from the structure (I) at the peak position (1.20 eV). A decay curve of the 3De–0Dh transition calculated by using equations (1)–(3) is fitted by a solid gray line. (b) Spectral dependence of the PL decay time in Ga(As)Sb QDs together with LTPL spectrum at an excitation density of 112 W cm^{-2}.

Figure 4(a) shows the decay curve from structure (I) at a photon energy of 1.19 eV together with the spectral response of the decay time. An excitation density is 112 W cm^{-2}, which is equivalent to the average carrier number in each QD of $\simeq$10. A decay time of the 3De–0Dh transition $\tau_{\rm BD} \simeq 30$ ns is observed from the 3De–0Dh transition and varies from $\simeq$30 to $\simeq$40 ns from the decay curves of the 3De–0Dh transition with different peak positions as shown in figure 4(b). The observed long decay time is likely due to the small overlap of the wavefunctions between electrons and holes which are physically separated because of the type-II nature. A long rise time can be observed from the 3De–0Dh transition although reduction of the rise time can be expected at such an extremely high excitation power due to the Auger processes [19]. In order to corroborate the carrier dynamics of type-II Ga(As)Sb QDs, 3-level rate equations for the holes are described as follows:

$$\frac{{\rm d}h_{\rm QD}}{{\rm d}t} = \frac{h_{\rm GaAs^*}}{\tau^*_{bd}} - \frac{h_{\rm QD}}{\tau_{\rm BD}} \tag{1}$$

$$\frac{{\rm d}h_{\rm GaAs^*}}{{\rm d}t} = \frac{h_{\rm GaAs}}{\tau_{\rm relax}} - \frac{h_{\rm GaAs^*}}{\tau^*_{bd}} - \frac{h_{\rm GaAs^*}}{\tau_{\rm GaAs}} \tag{2}$$

$$\frac{{\rm d}h_{\rm GaAs}}{{\rm d}t} = -\frac{h_{\rm GaAs}}{\tau_{\rm relax}} - \frac{h_{\rm GaAs}}{\tau_{\rm GaAs}} \tag{3}$$

where $h_{\rm QD}$, $h_{\rm GaAs^*}$ and $h_{\rm GaAs}$ are hole densities in Ga(As)Sb QDs, GaAs 2DEG and GaAs bulk, $\tau_{\rm relax}$ is a carrier relaxation time from GaAs bulk to GaAs 2D gas, and $\tau_{\rm GaAs}$ is a carrier decay time of the GaAs bulk–GaAs bulk transition. In order to consider the Pauli blocking in the ground state of Ga(As)Sb QDs, an effective capture time from GaAs to QDs, τ^*_{bd}, is defined as $\tau_{bd}/(1-P)$ where τ_{bd} is an intrinsic capture time, $P = h_{\rm QD}/2N_{\rm total}$ where $N_{\rm total}$ is a dot density. This rate-equation model includes the following relaxation and recombination processes: (i) electron–hole pairs are photo-generated by the pumping laser, (ii) photo-generated holes are diffused and captured into the GaAs 2D gas (which includes the effect of wetting layers of GaSb QDs for the simplification of rate-equation analyses) at a carrier relaxation time of $\tau_{\rm relax}$, (iii) holes captured into the GaAs 2D gas are relaxed into the QDs at an effective capture time of τ^*_{bd}, and (iv) radiative recombination processes of the holes in the GaAs 2D gas and QDs occur at carrier decay time of $\tau_{\rm GaAs}$ and $\tau_{\rm BD}$ for the GaAs bulk–GaAs bulk and 3De–0Dh transition, respectively. The obtained experimental result shown in figure 4(a) can be fitted by the rate equations (1)–(3) using the following parameters, $\tau_{\rm relax} = 1.5$ ns, $\tau_{\rm BD} = 30$ ns, $\tau_{\rm GaAs} = 5$ ns, and $\tau_{bd} = 3$ ns. From the analyses of rate equations, the observed long rise time can be explained by the Pauli blocking of holes from GaAs to QDs and a comparatively long τ_{bd} compared to that of type-I QDs ($\simeq$400 ps) [20].

Figure 5(a) shows the decay curves of the structure (II) with two different peak positions from the 2De–0Dh transition (1.08 eV) and the 3De–0Dh transition (1.19 eV) at an excitation density of 138 W cm^{-2}. An extremely long decay time of the 2De–0Dh transition, $\tau_{\rm WD} \simeq 50$ ns, is observed at a photon energy of 1.08 eV which originates from the 2De–0Dh transition. The observed longer $\tau_{\rm WD}$ compared to $\tau_{\rm BD}$ is

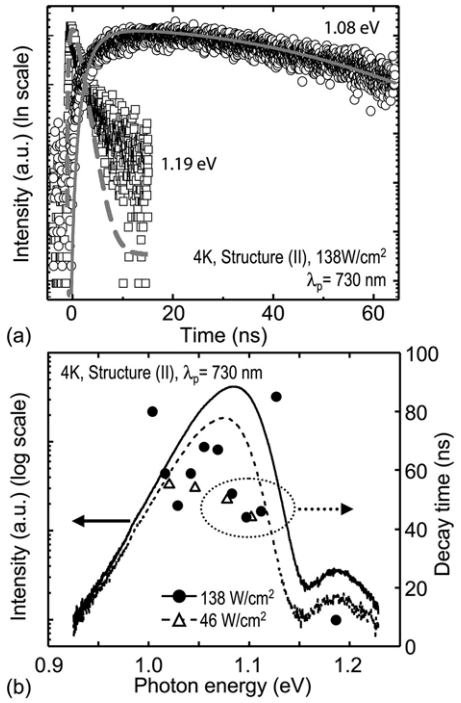

Figure 5. (a) Decay curves from the structure (II) with two different peak positions (1.08 and 1.19 eV) at an excitation density of 138 W cm^{-2}. Decay curves of the 2De–0Dh and 3De–0Dh transitions calculated by using equations (4)–(7) are fitted by solid and dashed gray lines, respectively. (b) Spectral dependence of the PL decay time together with LTPL spectrum at different excitation densities of 138 and 46 mW cm^{-2}.

likely due to the reduced overlap of the wavefunctions between electrons and holes because of the confinement of electrons in the QW [17]. In addition, the rise time from the 2De–0Dh transition of the structure (II) is longer than that of the 3De–0Dh transition of the structure (I). On the other hand, relatively smaller decay time of $\simeq$10 ns is observed from the 3De–0Dh transition. An inset shows the spectral dependence of the decay time with different excitation density of 138 and 46 W cm^{-2}, which are equivalent to the average carrier number in each QD of $\simeq$12 and $\simeq$4, respectively. The decay time varies from $\simeq$45 to $\simeq$70 ns from the decay curves of the 2De–0Dh transition with different peak positions as shown in figure 5(b). It is noted that almost the same decay time is obtained with different excitation densities. For comparison with the structure (I), 4-level rate equations are described as follows:

$$\frac{\mathrm{d}h_{\mathrm{QD}}}{\mathrm{d}t} = \frac{h_{\mathrm{QW}}}{\tau^*_{wd}} - \left(\frac{1}{\tau_{\mathrm{WD}}} + \frac{1}{\tau_{\mathrm{BD}}}\right) h_{\mathrm{QD}} \tag{4}$$

$$\frac{\mathrm{d}h_{\mathrm{QW}}}{\mathrm{d}t} = \frac{h_{\mathrm{GaAs}^*}}{\tau_{\mathrm{caph}}} - \left(\frac{1}{\tau^*_{wd}} + \frac{1}{\tau^*_{\mathrm{QW}}}\right) h_{\mathrm{QW}} \tag{5}$$

$$\frac{\mathrm{d}h_{\mathrm{GaAs}^*}}{\mathrm{d}t} = \frac{h_{\mathrm{GaAs}}}{\tau_{\mathrm{relax}}} - \frac{h_{\mathrm{GaAs}^*}}{\tau_{\mathrm{caph}}} - \frac{h_{\mathrm{GaAs}^*}}{\tau_{\mathrm{GaAs}}} \tag{6}$$

$$\frac{\mathrm{d}h_{\mathrm{GaAs}}}{\mathrm{d}t} = -\frac{h_{\mathrm{GaAs}}}{\tau_{\mathrm{relax}}} - \frac{h_{\mathrm{GaAs}}}{\tau_{\mathrm{GaAs}}} \tag{7}$$

where h_{QW} is a hole density of the InGaAs QW, τ_{caph} is a carrier relaxation time of holes from GaAs 2D gas to an InGaAs QW, and τ^*_{QW} is an effective carrier decay time of the 2De–2Dh transition. An effective capture time from QW to QDs, τ^*_{wd}, is defined as $\tau_{wd}/(1-P)$ where τ_{wd} is an intrinsic capture time from QW to QDs. This rate-equation model includes the following relaxation and recombination processes: (i) electron–hole pairs are generated by the pumping laser, (ii) photo-generated holes are diffused and captured into the GaAs 2D gas at a carrier relaxation time of τ_{relax}, (iii) holes captured in the GaAs 2D gas are relaxed into the QW at a capture time of τ_{caph}, (iv) holes captured in the QW are relaxed into the QDs at an effective capture time of τ^*_{wd}, and (v) radiative recombination processes of the holes in the GaAs 2D gas, QW and QDs occur at carrier decay time of τ_{GaAs}, τ^*_{QW}, τ_{BD} and τ_{WD} for the GaAs bulk–GaAs bulk, 2De–2Dh, 3De–0Dh and 2De–0Dh transition, respectively. The obtained experimental result shown in figure 5(a) can be fitted by the rate equations (4)–(7) using the following parameters, $\tau_{\mathrm{relax}} = 1.5$ ns, $\tau_{\mathrm{caph}} = 1.5$ ns, $\tau_{\mathrm{BD}} = 30$ ns, $\tau^*_{\mathrm{QW}} = 25$ ns, $\tau_{\mathrm{WD}} = 50$ ns, $\tau_{\mathrm{GaAs}} = 5$ ns, and $\tau_{wd} = 12$ ns. A larger τ^*_{QW} can be explained by the poor radiative efficiency of the 2De–2Dh transition resulting from the rapid relaxation of holes from QW to QDs, as indicated from the results of LTPL in figure 3. The observed longer relaxation time including τ_{bd}, τ_{wd}, τ_{caph}, or τ_{relax} can be caused by several factors: (i) carrier diffusion in the GaAs bulk [20], (ii) reduced relaxation process of holes by phonon-scattering processes due to the large valence band offset [21, 22], and (iii) suppression of the hole relaxation caused by Coulomb interactions and Auger processes [19]. In type-II QDs, suppression of the hole relaxation by the Coulomb interaction might dominantly affect the extremely longer τ_{bd} and τ_{wd} since the Coulomb interaction of excitons is much smaller than that of type-I QDs. It is also noted that the τ_{GaAs} and τ_{relax} obtained from the rate-equation analyses might not correspond to the actual values which are typically around the order of $\sim$100 ps and a few ps for τ_{GaAs} and τ_{relax}, respectively. It might be because the rate-equation analyses shown above might not be sufficient to elucidate these reasons. Further analyses and investigation will be required to understand the detailed carrier relaxation mechanism of type-II QD in a type-I QW.

4. Conclusions

In summary, we report the optical properties and carrier dynamics of Ga(As)Sb/GaAs QDs embedded in an InGaAs QW. A large blueshift of the PL which is characteristics of the type-II band alignment is observed by increased excitation density. This is caused by the Coulomb interaction between electrons and holes which are physically separated and a band-filling effect of the electrons confined in the QW. LT-TRPL measurements describe much longer decay time of $\simeq$40–70 ns from the 2De–0Dh transition than that of the 3De–0Dh transition ($\simeq$30 ns), which is likely due to the reduced overlap of the wavefunction between electrons and holes.

Acknowledgments

This work is supported by the Air Force Office of Scientific Research (FA9550-06-1-0407) under Gernot Pomrenke and Kitt Rheinhardt. Low-temperature time-and frequency-resolved PL studies reported here are conducted at the Center for Integrated Nanotechnologies, jointly operated for US Department of Energy by Los Alamos and Sandia National Laboratories. The authors would like to thank A Khoshakhlagh for her support of MBE growth operations.

References

[1] Sai-Halasz G A, Chang L L, Welter J M, Chang C A and Esaki L 1978 *Solid State Commun.* **27** 935
[2] Kroemer H and Griffiths G 1983 *IEEE Electron Device Lett.* **EDL-4** 20
[3] Arakawa Y and Sakaki H 1982 *Appl. Phys. Lett.* **40** 932
[4] Hatami F *et al* 1995 *Appl. Phys. Lett.* **67** 656
[5] Bennett B R, Shanabrook B V and Magno R 1996 *Appl. Phys. Lett.* **68** 958
[6] Sun C-K, Wang G, Bowers J E, Brar B, Blank H-R, Kroemer H and Pilkuhn M H 1996 *Appl. Phys. Lett.* **68** 1543
[7] Glaser E R, Bennett B R, Shanabrook B V and Magno R 1996 *Appl. Phys. Lett.* **68** 3614
[8] Hatami F *et al* 1998 *Phys. Rev.* B **57** 4635
[9] Suzuki K, Hogg R A and Arakawa Y 1999 *J. Appl. Phys.* **85** 8349
[10] Farrer I, Murphy M J, Ritchie D A and Shields A J 2003 *J. Cryst. Growth.* **251** 771
[11] Balakrishnan G, Tatebayashi J, Khoshakhlagh A, Huang S H, Jallipalli A, Dawson L R and Huffaker D L 2006 *Appl. Phys. Lett.* **89** 161104
[12] Tatebayashi J, Khoshakhlagh A, Huang S H, Dawson L R, Balakrishnan G and Huffaker D L 2006 *Appl. Phys. Lett.* **89** 203116
[13] Tatebayashi J, Khoshakhlagh A, Huang S H, Balakrishnan G, Dawson L R, Huffaker D L, Bussian D A, Htoon H and Klimov V 2007 *Appl. Phys. Lett.* **90** 261115
[14] Motlan M and Goldys M E 2001 *Appl. Phys. Lett.* **79** 2976
[15] Geller M, Kapteyn C, Müller-Kirsch L, Heitz R and Bimberg D 2003 *Phys. Status Solidi* b **238** 258
[16] Gradkowski K, Ochalski T J, Williams D P, O'Reilly E P, Huyet G, Tatebayashi J, Khoshakhlagh A, Balakrishnan G, Dawson L R and Huffaker D L 2008 *SPIE Photonic West* **6902** 17
[17] Madureira J R, De Godoy M P F, Brasil M J S P and Iikawa F 2007 *Appl. Phys. Lett.* **90** 212105
[18] Laghumavarapu R B, Moshco A, Khoshakhlagh A, El-Emawy M, Lester L F and Huffaker D L 2007 *Appl. Phys. Lett.* **90** 173125
[19] Bockelmann U and Egeler T 1992 *Phys. Rev.* B **46** 15574
[20] Adler F, Geiger M, Bauknecht A, Scholz F, Schweizer H, Pilkuhn M H, Ohnesorge B and Forchel A 1996 *J. Appl. Phys.* **80** 4019
[21] Benisty H, Sotomayor-Torrès C M and Weisbuch C 1991 *Phys. Rev.* B **44** 10945
[22] Bockelmann U 1993 *Phys. Rev.* B **48** 17637